(ANPA Conference 2025)
ISSN: 2392-473X(Print), 2738-9537 (Online)

Research Article ©Nepal Physical Society
DOI: https://doi.org/10.3126/jnphyssoc.v11i1.87461

Boosting Swiss Chard Germination with Atmospheric Pressure Plasma Jet

Bablu K. Thakur,[1] Arun K. Shah,[2] Ram L. Sah,[1,2] Reeta Silpakar,[1,2] Rajendra Shrestha,[1,2] and Lekha N. Mishra[1,3,a)]

[1)] *Department of Physics, Tri-chandra Multiple Campus, Tribhuvan University, Kathmandu, 44600, Nepal*
[2)] *Department of Physics, Patan multiple campus, Tribhuvan University, Lalitpur, 44700, Nepal*
[3)] *Department of Physics, Nepal Banepa Polytechnic Institute, Banepa, 45210, Nepal*

[a)] *Corresponding author:lekha.mishra@pmc.tu.edu.np*

Abstract. This study was carried out to reveal the effect of non thermal atmospheric pressure plasma jet on germination of Swiss chard seed. The Atmospheric Pressure Plasma Jet has been characterized by electrical and optical methods. The electron density and electron temperature have been determined by power balance, and Boltzmann plot method respectively. A cold APPJ with argon gas source was employed in this study. APPJ has been generated using high voltage power supply (0 - 20 KV) and high frequency (27 MHz). The electron density was found to be $1.68 \times 10^{20} m^{-3}$ and average electron temperature was estimated to be 0.73 eV. The effects of different duration of plasma jet on germination of the Swiss chard seed was studied. The Swiss chard seed was treated by plasma for different duration of time.

Received: August 10, 2025; **Revised**: October 2, 2025; **Accepted**: October 29, 2025

Keywords: Electrical characterization; Optical characterization; Germination; Voltage; Frequency

1. INTRODUCTION

If external energy is applied to a solid, it is converted to liquid which becomes gas upon the addition of more energy. Energy is applied further so that electrons are detached from gas atom. Once ionized, the gas's dynamic behavior is affected by external electric and magnetic fields. This is because the ionization causes a separation of charges, making the properties of the gas distinct from those of neutral atoms. This ionized state of matter was termed plasma by Langmuir [1]. The plasma shows collective behavior because the motion of charged particles not only depends on local conditions but also on state of the plasma in remote regions. The plasma is quasi-neutral because of the density of ionized atoms (n_i) $\approx$ electron density (n_e) $\approx$n (plasma density). [2]. Various atmospheric pressure and low-pressure plasma systems have been developed. Low-pressure plasmas, in particular, are widely used in applications such as thin film deposition, substrate cleaning, and the surface treatment of polymers [3]. In non-thermal plasma, electrons possess a higher temperature compared to ions, yet the overall temperature of the plasma remains relatively low. Atmospheric pressure plasma plays a vital role as a fundamental tool in facilitating various chemical reactions at low temperatures [4]. The plasma jet is analyzed both electrically and optically, particularly in relation to the applied voltage and frequency. Due to the low operating voltage of atmospheric pressure plasma jets (APPJ), they are considered safe for human exposure [5]. Optical emission spectroscopy is used to measure the electron temperature, while the electron density is evaluated using the power balance method [6]. Cold atmospheric pressure plasma is widely used in industry to enhance surface hydrophilicity and to modify surface characteristics [7]. Additionally, cold atmospheric pressure plasma jets have extensive applications in the medical field [8]. Plasma treatments influence the wetting behavior of surfaces [9]. These treatments alter the surface roughness, which in turn affects the surface's wettability [10]. Plasma treatment has been shown to enhance seed germination rate, surface wettability, water uptake, and crop yield [11, 12, 13]. Traditional chemical methods were costly and contributed to soil pollution. In contrast, cold plasma treatment causes minimal damage to seeds, as the APPJ generally penetrate only a few nanometers [14], resulting in minimal environmental pollution.

Swiss chard (Beta vulgaris L.), a leafy vegetable, is known for its high nutritional value. It is widely favored in many parts of the world for its health benefits, affordability, and culinary versatility [15]. Its stalks and leaves are rich in vitamins A, B, and C, and minerals like calcium, phosphorus, and iron [16]. When cooked, the leaves provide 20 kcal per 100 grams [17]. This vegetable has valuable traits that can significantly support food security efforts, particularly in combating malnutrition [18].

This paper presents the application of cold atmospheric pressure plasma jet for promoting seed germination.

2. EXPERIMENTAL METHODS

2.1 Sample collection

The Swiss chard seeds were obtained locally from Kathmandu Market. The Swiss Chard was kept in petri dish and the seed was treated by plasma. Then, untreated and treated seeds were sowed in seed tray filled with soil. There were 50 cells in each tray. In each cell, one seed was sowed. For treating seed with plasma, seeds of similar size were taken.

2.2 Plasma generation and its characteristics

The plasma treatment of Swiss chard seeds was performed by cold atmospheric plasma jet. The cold atmospheric pressure plasma jet system consists of dielectric electrodes, high voltage power supply, voltage controller and Argon gas. This power supply is used in order to cut the overall cost of the device by replacing the expensive RF power supply. The power supply has an output of 8 kV voltage, 30 mA current and 27 MHz frequency. The input of this power supply is 220 V. The voltage controller regulates the primary voltage of the high voltage transformer. The electrode system consists of quartz glass tube of thickness 0.2 cm and length 13 cm. The electrons 1.5cm wide are made of aluminum foil. The gas flow system is responsible for delivering the gas to the plasma jet. It consists of the gas storage cylinder, gas flow regulators and rubber hose. In this study Argon gas was used to test the plasma jet operation. Argon is introduced through the quartz glass and high voltage AC Power is applied, the plasma is generated between two electrodes. The voltage applied to Argon gas ionizes Argon gas atoms. Free electrons course further ionization of neighbouring Argon atoms by collision. This series of reactions convert the Argon gas to the plasma which is different from solid, liquid and gas states. Hence this device generates room temperature and atmospheric pressure plasma and extends up to 1.6 cm. The experimental set up to produce plasma jet is shown in Figure. 1 The flow rate for argon gas

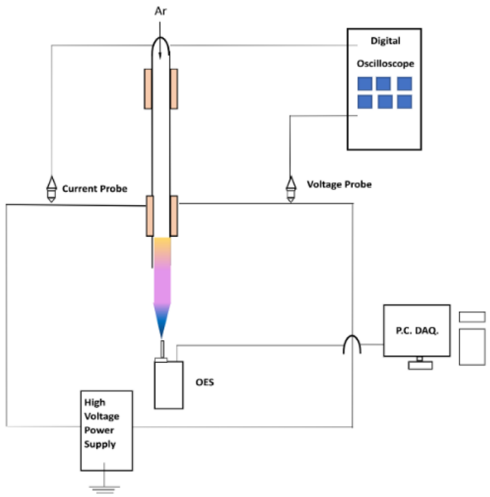

FIGURE 1: Schematic Diagram of Plasma jet

is 2 litre/min and the voltage and frequency were 8 kV and 50 MHz respectively. The electrical characterization of the discharge was also done by measuring the current and voltage waveforms were analyzed in TEKTRONIX TBS 2002 Oscilloscope by using current probe and voltage probe (PINTEX HVP-28HF). The attenuation ratio of the voltage probe is 1000:1. Similarly, optical characterization of the discharge was done by using line Boltzmann plot method with the help of OES. (USB 2000 + Ocean Optics) Materials used for the electrical and optical characterization of atmospheric pressure plasma jet is shown in Figure 2.

3. RESULT AND DISCUSSION

3.1. Electrical Characterization of APPJ

Figure 3(a) shows the discharge current with respect to time and 3(b) shows the discharge voltage with respect to time of APPJ, with electrode gap of 50 mm, applied voltage 8 kV and an operating frequency of 50 MHz at atmospheric pressure condition. The electron density is determined by using power balance method expressed in eqn.(1) [19], [20].

$$n_e = \frac{P_{ab}}{2AV_bE_{\text{lost}}}, \tag{1}$$

where P_{ab} is the total power absorbed, A is the area of electrode, V_b is the Bohm velocity and E_{lost} is the energy lost per cycle [21].

FIGURE 2: (a) Plasma treating on Seed, (b) Power supply, (c) Digital oscilloscope, (d) Chlorofillmeter

The following parameters were used in the calculation: $V_b = 2 \times 10^3$ m/s, $E_{\text{lost}} = 80 \times 10^{-19}$ J, $A = 3.77 \times 10^{-5}$ m^2, $V = 8$ kV, and $I = 20$ mA. The electron density was found to be 1.68×10^{20} m^{-3} [21], [22], [23].

This method is based on balance between energy lost by plasma components and energy gained by plasma from applied plasma sources.

3.2 Optical Characterization of APPJ

Boltzmann Plot Method: The electron temperature can be calculated by using Boltzmann plot with eqn(2) [24]

$$\ln\left(\frac{I_{ki}\lambda_{ki}}{hcg_kA_{ki}}\right) = -\frac{E_k}{K_BT_E} + C, \qquad (2)$$

where I_{ki} is the relative intensity of chosen spectral lines, λ_{ki} is the wavelength, g_k is the statistical weight, E_k is the excitation energy, k_B is the Boltzmann constant, and C is a constant for all selected spectral lines.

In our work, for wavelength range of 696.54 nm to 811.53 nm, four Ar I with wavelength 696.54 nm, 751.46 nm, 763.51 nm, and 810.36 nm respectively were chosen to calculate the electron temperature of atmospheric pressure plasma jet are Boltzmann plot method. The atomic data for four Ar I lines are shown in table given below.

The graph of $\ln\left(\frac{I_{ki}\lambda_{ki}}{g_kA_{ki}}\right)$ versus E_k is shown in Figure 5. The slope of the straight line gives the electron temperature.

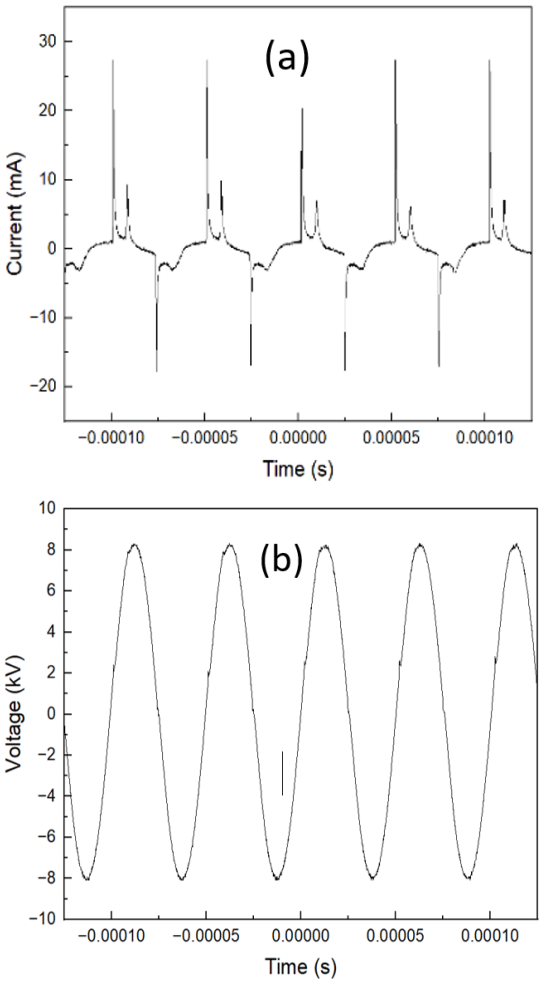

FIGURE 3: (a) Current-Time Graph, (b) Voltage-Time Graph

TABLE I: Spectral line parameters used for analysis.

λ_{nm}	A_{ki} (s^{-1})	E_k (eV)	g_k
696.54	6.4×10^6	13.327	3
751.46	4.0×10^7	13.273	1
763.51	2.45×10^7	13.171	5
810.36	2.50×10^7	13.151	3

The electron temperature was found using the formula: $T_e = \frac{1}{mK_B}$, where m is the slope $[m = -1.43]$ and $K_B = 8.617 \times 10^{-5}$ eV/K. The electron temperature calculated using the Boltzmann plot was found to be 0.73 eV.

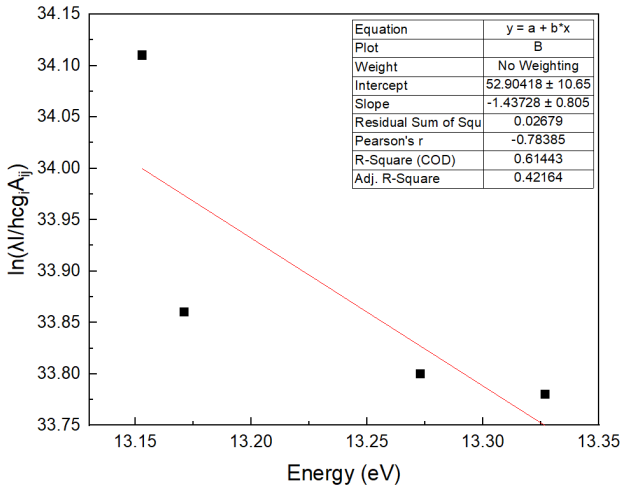

FIGURE 4: Boltzmann plot method for determination of electron temperature

3.3 FTIR

Fourier Transform Infrared Spectroscopy was conducted by utilizing the spectrum two model. There were four scans. MIRTGS was the detector and MIR was the source. The scan range was 450 $cm^{-1} - 5000\ cm^{-1}$. FTIR was used in Amrit Science College in Kathmandu. FTIR is used to measure infrared light by a sample.

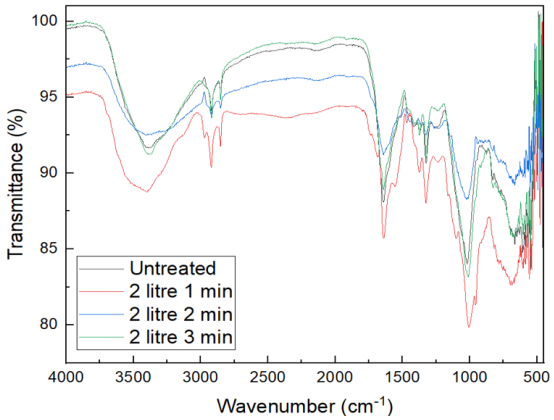

FIGURE 5: FTIR Spectra (Untreated and Treated Seeds) and gas flow at rate of 2 litre/min.

The FTIR analysis of untreated and cold plasma treated Swiss chard in an argon environment is shown in Figure 5. The absorption peak is a result of the stretching of functional groups such as C-H, C-O bonds at different wavenumbers. Tables II, III, and IV show identification of functional groups based on the absorbance peak with respect to wavenumber. It was seen that transmittance decreases slightly in treated seeds compared to untreated seeds. The stretching of functional group refers to a type of molecular vibration where the bond length between atoms in a functional group increases and decreases periodically, like a spring. The change in bond length varies with the functional group, causing the variation in transmittance. Further analysis of transmittance of IR through different functional group revealed that functional group of CH-Bond, C=O Bond, N=O Bond and C-O bond of 1 minute treated seed at the gas flow rate of 2 litre/min decreases that untreated seeds by 2.9%, 1.69%, 4.65%, 2.36%, 2.85%, 4.16% and 3.04%. For gas flow rate of 2 litre, transmittance of 2 minute treated seed OH bond, C=O Bond, C-N bond increases by 0.84%, 3.07% and 0.44% respectively, but that of CH_2 group decreases by 0.31% and (2850 – 2854) decrases by 0.74%. For gas flow rate of 2 litre, treating plasma for 3 minutes, the transmittance of IR through OH Group, CH group, CH_2 group, CN group and C-O group decreased by 0.43%, 0.45%, 0.16%, 0.02% and 0.86% respectively, but that of C=O group increased by 0.52%. The change in transmittance may cause to increase the germination of seed. Also, for the gas flow rate of 2 litre, treating plasma on seed for 1 minute, CH_2 and C-O group is added and for same flow rate of 2 minute treated seed, CH_3.

Germination of Swiss Chard

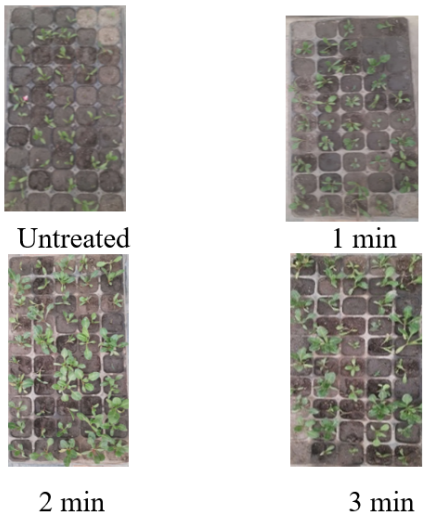

FIGURE 6: Germination of Untreated and Treated Seeds

Figure 7 shows the germination rate of treated and untreated seeds. The germination percentage of untreated Swiss chard was found to be 66%. However, the germination percentage of the treated seeds and gas flow rate was 2 litre/min was found to 80%, 92%, 92% for 1 minute, 2 minutes and 3 minutes respectively. The percentage of seeds that germinate rises when they are treated with plasma. However, the amount of seed germination in-

TABLE II: Comparison and identification of functional group present on Swiss chard seed [25], [26]

Absorption Peak (cm^{-1})	**Functional Group**	**Untreated**	**2l, 1m**	**2l, 2m**	**2l, 3m**
3397–3402	OH – Group (Hydroxyl Compound)	91.65	88.75	92.49	91.22
2918–2919	CH_2 (C–H, Aliphatic Compounds)	94.08	92.39	93.77	93.63
2850–2854	CH_2 (Aliphatic Compounds)	95.04	90.39	94.30	94.88
1643–1648	C=O (Ketonic Compound)	88.08	85.72	91.15	88.90
1371–1376	C=N (Aromatic Amine)	92.97	90.12	93.41	92.25
1003–1016	C–F (Aliphatic Compound)	84.02	79.86	–	83.16
664–696.53	Aliphatic Compound	85.68	82.64	89.15	85.70

TABLE III: Functional Group Added after treating seed

Parameter	**2l, 1 min**
Wavenumber (cm^{-1})	2974, 1241 and 1103
Functional Group	CH_2 , C-O

TABLE IV: Functional Group Lost after treating seed

Parameter	**2l, 2 min**
Wavenumber (cm^{-1})	1376
Functional Group	CH_3

crease varies depending on the seed and the duration of plasma treatment. This is consistent with earlier research. [27], [28], [29]

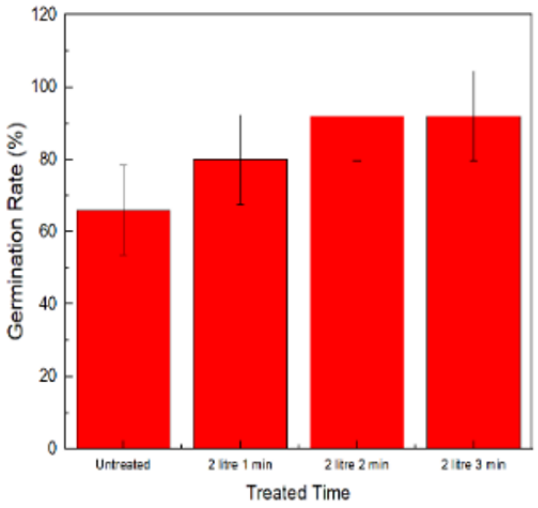

FIGURE 7: Germination rate for untreated and treated seeds

Figure 8 shows the chlorophyll content of treated and untreated seeds. The leaf of plant was kept in chlorofillmeter as shown in the figure 2(d). The values of chlorophyll is displayed on screen of chlorophyll meter. The

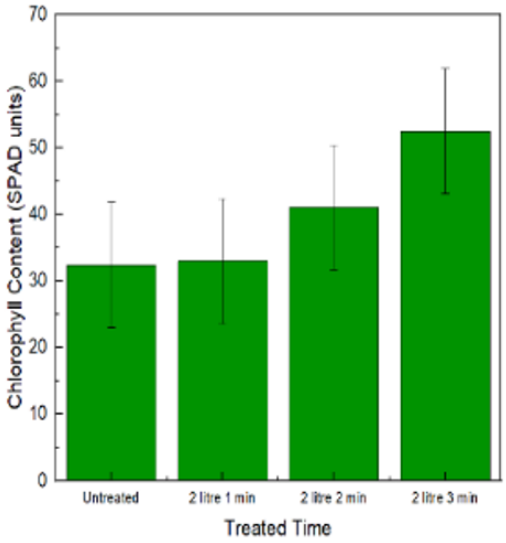

FIGURE 8: Chlorophyll content for untreated and treated seeds

unit of chlorophyll is SPAD (Soil Plant Analysis Development). SPAD is relative index of chlorophyll content in a leaf. Higher values of SPAD indicates more chlorophyll content. Chlorophyll content was 32.38 for untreated seeds. It was found to be 32.99, 41.06, and 52.5 for 1 minute, 2 minute and 3 minutes treated seed respectively. The cold atmospheric plasma jet can alter germination rate and chlorophyll content. This is in agreement with the previous work. [30]

5. CONCLUSION

Cold Atmospheric Pressure Plasma Jet has been produced and characterized by electrical and optical methods. Electron density by electrical method was found to be 1.68 x 10^{20} m^{-3}. Also, by Boltzmann plot method, the electron temperature was found to be 0.73 eV, the germination percentage of treated seed was found to be in-

creased. Also, the chlorophyll content of the treated seeds was found to be increased than that of untreated seeds. It can be concluded that APPJ has positive impact on seed and is expected to be used in the future.

EDITORS' NOTE

This manuscript was submitted to the Association of Nepali Physicists in America (ANPA) Conference 2025 for publication in the special issue of the Journal of Nepal Physical Society.

REFERENCES

1. I. Langmuir, Oscillations in Ionized Gases. Proc Natl Acad Sci U S A. 1928 Aug;14(8):627-37.
2. F. F. Chen, *Introduction to Plasma Physics*, (Springer, Boston, 1984).
3. M. Konuma, *Film Deposition by Plasma Techniques*, Springer Series on Atomic, Optical, and Plasma Physics, Vol. 10, (Springer, Berlin, 1992).
4. J. R. Roth, *Industrial Plasma Engineering, Vol. 2: Applications to Non-Thermal Plasma Processing*, (IOP Publishing, Bristol and Philadelphia, 2001).
5. A. Hamdan, J.-L. Liu, and M. S. Cha, "Microwave plasma jet in water: characterization and feasibility to wastewater treatment," Plasma Chem. Plasma Process. **38**, 1003–1020 (2018).
6. S. Fester, C. Mohr, and W. Viöl, "Investigations of atmospheric pressure plasma jet by optical emission spectroscopy," Surf. Coat. Technol. **200**, 827–830 (2005).
7. D. L. Pavia, G. M. Lampman, and G. S. Kriz, *Introduction to Spectroscopy*, 3rd ed., Sanat Printers (2001). `https://trove.nla.gov.au/work/8887496`
8. M. Ŝimor, J. Ráheľ, P. Vojtek, et al., "Atmospheric-pressure diffuse coplanar surface discharge for surface treatments," Appl. Phys. Lett. **81**, 2716–2718 (2002).
9. J. F. Kolb, A.-A. H. Mohamed, R. O. Price, et al., "Cold atmospheric pressure air plasma jet for medical applications," Appl. Phys. Lett. **92**, 241501–241503 (2008).
10. R. M. France and R. D. Short, "Plasma treatment of polymers: the effects of energy transfer from an argon plasma on the surface chemistry of polystyrene and polypropylene," Langmuir **14**, 4827–4835 (1998).
11. R. Molina Canal, E. Bertran, and P. Erra, "Study on the influence of scouring on the wettability of keratin fibers before plasma treatment," Fibers Polym. **9**, 444–449 (2008).
12. M. Dhayal, S.-Y. Lee, and S.-U. Park, "Application of low-temperature substrate bonding in fabrication of reusable microfluidic devices," Vacuum **80**, 499–506 (2006).
13. E. Bormashenko, R. Grynyov, Y. Bormashenko, and E. Drori, "Cold radiofrequency plasma treatment modifies wettability and germination speed of plant seeds," Sci. Rep. **2**, 741 (2012).
14. M. Q. Yin, M. G. Huang, B. Z. Ma, et al., "Stimulating effects of seed treatment by magnetized plasma on tomato growth and yield," Plasma Sci. Technol. **7**, 3143–3147 (2005).
15. F. Denes, S. Manolache, and R. A. Young, "Synthesis and surface functionalization under cold-plasma conditions," J. Photopolym. Sci. Technol. **12**, 27–38 (1999).
16. Z. J. Gao, X. H. Han, and X. G. Xiao, "Purification and characterization of polyphenol oxidase from red Swiss chard (Beta vulgaris subsp. cicla) leaves," Food Chem. **117**, 342–348 (2009).
17. Y. Pyo, T. Lee, L. Logendra, et al., "Antioxidant activity and phenolic compounds of Swiss chard (Beta vulgaris subsp. cicla) extracts," Food Chem. **85**, 19–26 (2004).
18. B. E. van Wyk, *Food Plants of the World: Identification, Culinary Uses and Nutritional Value*, 1st ed. (Briza Publications, Pretoria, South Africa, 2005).
19. H. Gebremedhin and H. Awgechew, "The response of Swiss chard (Beta vulgaris L.) to nitrogen levels and intra-row spacing in Debre Berhan, Central Ethiopia," J. Hortic. Postharvest Res. **2**(2), 105–116 (2019).
20. K. K. Trusov, "Dynamics of multichannel and quasi-homogeneous sliding discharge formation in rare gases," J. Phys. D: Appl. Phys. **40**, 786–794 (2007).
21. A. Kramida, Y. Ralchenko, J. Reader, and NIST ASD Team, *NIST Atomic Spectra Database*, `https://physics.nist.gov/asd` (2018) [accessed March 14, 2019].
22. D. Lingegowda, K. D. Kumar, A. G. Devi Prasad, M. Aarei, and S. Gopal, "FTIR spectroscopic studies on Cleome gynandra – comparative analysis of functional group before and after extraction," Rom. J. Biophys. **22**(3–4), 137–143 (2012).
23. D. Samargandi, X. Zhang, F. Liu, and S. Tian, "Fourier Transform Infrared (FT-IR) spectroscopy for discrimination of fenugreek seeds from different producing areas," J. Chem. Pharm. Res. **6**(9), 19–24 (2014).
24. A. D. Valiño, A. Elias, M. Rodríguez, and N. Albelo, "Evaluation using Fourier Transformed-Infrared spectroscopy (FTIR) of biodegradation by the strain Trichoderma viride M 5-2 from the cell walls of sugarcane (Saccharum officinarum Lin) bagasse pretreated," Int. J. Chem. Biomol. Sci. **1**(3), 134–140 (2015).
25. G. Theivandran, I. S. Mohamed, and M. Murugan, "Fourier Transform Infrared (FT-IR) spectroscopic analysis of Spirulina fusiformis," J. Med. Plants Stud. **3**(4), 30–32 (2015).
26. J. O. Lopes, R. A. Garcia, and N. D. Souza, "Infrared spectroscopy of the surface of thermally-modified teak juvenile wood," Maderas Cienc. Tecnol. **20**(4), 737–746 (2018).
27. K. Lotfy, Effects of Cold Atmospheric Plasma Jet Treatment on the Seed Germination and Enhancement Growth of Watermelon. *Open Journal of Applied Sciences*, **7**, 705-719 (2017).
28. B. K. Thakur, A. K. Shah, R. L. Sah, R. Silpakar, R. Shrestha, & L. N. Mishra, Plasma jet therapy on seeds for improvement of germination and development. *International Journal of Plasma Environmental Science and Technology*, 19(1), e01001 (2025).
29. A. K. Shah, S. H. Dhobi, R. L. Sah, R. Shrestha, L. N. Mishra, & J. J. Nakarmi, Impact of Plasma Treatment on Lady's Finger Seeds for Germination and its Growth. *Journal of Nepal Physical Society*, *9*(1), 107–115 (2023).
30. P. Attri, K. Ishikawa, T. Okumura, K. Koga, M. Shiratani, Plasma Agriculture from Laboratory to Farm: A Review. Processes. 8(8), 1002 (2020).